MICROWAVE TEST CHAMBER FOR MEASURING THE RELATIVE PERMITTIVITY OF THIN FILMS

A Thesis

Presented to

The Faculty of Graduate Studies and Research

The University of Manitoba

In Partial Fulfillment

of the Requirements for the Degree

Master of Science

in

Electrical Engineering

by

Harinder Pal Singh Ahluwalia

September, 1970

ACKNOWLEDGEMENTS

I wish to express my gratitude to Dr. W.M. Boerner under whose able guidance the project was conducted. I am pleased to acknowledge my indebtedness to Professor M.A.K. Hamid and Dr. S.S. Stuchly for many fruitful discussions and to Dr. A. Petkau of Atomic Energy of Canada Ltd. for his encouragement and for supplying the test films. I also wish to thank Dr. C.W. Searle of the Physics Department for his assistance in component fabrication and Mr. Bodo Meyer of the Physics Workshop for his skilled and precise machining of the test chamber.

Last but not the least, I am particularly appreciative of the tireless efforts of Miss. A.M. Korol for careful and cheerful typing of this material.

This research was supported by the National Research Council of Canada, the Defence Research Board of Canada and the Faculties of Agriculture and Graduate Studies of the University of Manitoba.

(H.P.S. Ahluwalia)

CONTENTS

LIST OF FIGURES

LIST OF TABLES

LIST OF PHOTOGRAPHS

Abstract

A microwave test chamber for measuring the dielectric constant of thin films on substrates using the cavity perturbation technique is described. Special emphasis is placed on testing biochemical phospho-lipid membranes, whose properties resemble those of living tissues; therefore their rupture by microwave irradiation may determine microwave safety levels. A novel feature of the test chamber is the use of a resonant iris to enhance the field in the aperture where the sample is suspended. It is shown that significant shift in the center frequency and change in the Q factor of the X-band cavity are obtained for films of thicknesses as low as a few hundred microns.

CHAPTER I

INTRODUCTION

The work presented here resulted from a fundamental research on rf safety standards to establish criteria for defining the transition between macro and micro-thermal effects on tissue layers caused by electromagnetic irradiation. The behaviour of such membranes at high power densities is of particular importance since the power density at which they rupture is an indication of the critical level which may determine the safety standard for microwave irradiation [1]. The study is being carried out on artificial phospho-lipid membranes which resemble living tissues very closely in their chemo-physical properties [2]. It may also be possible to electrically bias the two bipolar membrane layers and to create membranes of electro-active properties by proper ion doping of the two bipolar phospho-lipid membrane layers.

Although the basic incentive of this research is to study the rupture of biochemical membranes and their electrical permittivity, the test chamber described in this work may also be used for dielectric measurements of samples of different semiconductor materials. These measurements at microwave frequencies enable one to deduce information regarding the properties of carriers not obtained by dc techniques. Even in those cases where the properties can be determined by dc as well as microwave techniques, the latter have the advantage of not requiring contacts ,thus eliminating the possiblity of altering the sample characteristics during the measurement. It has been shown [3] that for semiconductors, the conductivity measured at microwave frequencies is the same as the dc conductivity but the dielectric constant obtained by microwave measurements differs from the dc value by $\sigma_s \tau/\varepsilon_o$. Here σ_s is the microwave conductivity, τ the momentum relaxation time and ε_o the free space permittivity. Furthermore, measurement of the complex permittivity as a function of frequency and temperature yields information on the scattering mechanisms controlling the transport of charge carriers.

A number of methods for measuring the dielectric constant of semiconductors using substitution, standing wave ratio, transmission bridge, and resonant cavity techniques have been described in the literature [4-7]. However none of these methods is applicable to thin films of thicknesses in the range of a few hundred microns deposited on substrates. It should be noted that the study of microwave properties of thin films of semiconductors has been of increasing importance due to their potential application in microwave devices. Attempts are being made to increase the frequency range of transistors and other semiconductor devices. One of the main limiting factors in the construction of transistors to operate at higher frequencies is the base width which has to be extremely small, thus approximating a thin film. Since the dielectric constant of such thin films is anticipated to be considerably different from the tabulated bulk value, the technique described in this thesis could be suitable for such studies.

The cavity perturbation method has been found suitable for the measurement of the dielectric constant of thin films. The measurement is performed by inserting the sample film into a cavity resonator and determining the properties of the sample from the resultant change produced in the resonant frequency and the quality factor of the cavity. The aim of the present scheme is to create a high electric field in the plane of the sample in order to enhance the changes in the measured quantities. For this the sample is suspended in a resonant iris which is placed at the maximum longitudinal field in a resonant rectangular cavity. The measured shift in the resonant frequency and Q factor of the cavity are utilized in the perturbation equation to determine the complex permittivity.

CHAPTER II

MEASUREMENT TECHNIQUE

A variety of methods for measuring dielectric constants are available [4-8]. Since it is required to measure the dielectric constant of 'thin' films, the conventional methods based on transmission and reflection of power in a waveguide, containing a sample approximately a quarter wavelength long, cannot be employed. In this case the cavity perturbation method,which is highly sensitive and versatile with regard to the type and shape of the sample,is suitable. When the perturbation method is used in conjunction with the quasi static approximation,the accuracy of the results may be surprisingly high. Since the cavity perturbation methods involve approximations in their formulation, the sample to be tested has to satisfy certain conditions. The sample must be very small, compared with the cavity itself,so that the induced frequency shift and change in Q are small compared with the centre frequency and Q of the unloaded cavity and also for the quasi-static approximation to be valid. Our thin films satisfy the above requirements thus justifying the use of the cavity perturbation technique. A great advantage of the perturbation approach is that it is no longer necessary to account for many of the details of the cavity which are the same for the loaded and unloaded cases and hence their effect is cancelled out.

The change in the Q factor and resonant frequency due to the sample are utilized to calculate ε_r using the perturbation equation:

$$\frac{f_o - f_s}{f_s} - j \left(\frac{1}{Q_o} - \frac{1}{Q_s} \right) = (\varepsilon_r - 1) \frac{\int_{V_s} \vec{E}_o \cdot \vec{E}_2 \, dv}{\int_V |\vec{E}_o|^2 \, dv} \qquad (1)$$

Here f_o and Q_o are the resonant frequency and quality factor for the unloaded cavity, respectively, whereas f_s and Q_s are the corresponding quanitities for the loaded cavity. $\vec{E}_o$ is the transverse electric field in the unloaded cavity volume v_o and $\vec{E}_2$ is the electric field in the sample volume V_s.

When the sample extends over the entire cross-section, and is tangential to the electric field, $\vec{E}_2 = \vec{E}_o$ for small perturbations. How ever, when the sample is suspended in the iris aperture only, it is more difficult to determine $\vec{E}_2$ with satisfactory accuracy since the field distribution in such a resonant aperture is not available. A resonable estimate for this field may be obtained with the aid of a shape factor γ which is determined experimentally using films with precisely known dielectric constants as discussed later.

There are two general methods for the measurement of Q of a cavity. One method depends on observing the response of the resonator to CW signals in the neighborhood of its resonant frequency and the other involves observing the transient response of the resonator to the sudden application or removal of an exciting signal at or near resonant frequency. The first method includes a number of different measurement techniques such as transmission methods, impedance measurement method and dynamic methods. The transient decay or the decrement method is particularly applicable to high Q cavities because it does not need a high degree of frequency stability required in other types of measurements, but at lower values the decay period is too short for convenient measurement. In the present measurements, the reflectometer method which applies particularly to .e single-ended resonators was found to be convenient because it lends itself readily to oscilloscopic presentation and has the advantage of speed.

The reflectometer method simply requires the measurement of the voltage reflection coefficient $|\rho_o|$ at the resonant frequency f_o and at two other frequencies f_1 and f_2, symmetrically spaced about f_o. If there are appreciable losses in the input coupling structure, the reflection coefficient magnitude $|\rho_1|$ far from resonance must also be measured. The Q of the resonator is then given by the relation:

$$Q_L = \frac{\alpha f_o}{\Delta f} \tag{2}$$

where $$\Delta f = f_2 - f_1 \tag{3}$$

and $$\alpha = \left[\frac{|\rho|^2 - |\rho_o|^2}{|\rho_1|^2 - |\rho|^2} \right]^{1/2} \tag{4}$$

CHAPTER III

TEST CHAMBER

The microwave test chamber consists of an X-band rectangular cavity operated in TE_{10n} mode and coupled to the main waveguide through a circular iris. The radius of the iris is such that the cavity is critically coupled to the main waveguide. A sliding short is employed to vary the cavity length as shown in Fig. 2. Two requirements need to be satisfied simultaneously, the first is to create a high electric field in the applicator along the sample and the second is to place the sample in the region where the highest electric field values exist. The need to create a high electric field in the sample arises from the fact that films of a few micron thickness, when suspended in the total cross section of the cavity, induce a very small perturbation in the complex frequency (obtained from the resonant frequency and the Q factor of the cavity). By suspending the films in a resonant iris, and thus enhancing the electric field in the sample, an increase in the change of complex frequency is obtained. The requirements mentioned above are satisfied by placing the resonant iris, containing the sample, an odd multiple number of quarter wavelengths away from the sliding short. Since the frequency perturbation for thin films is generally small, utmost care must be exercised in very accurate machining of the various components of the chamber. Furthermore special care must be taken during the experiment to align the chamber assembly in both transverse and longitudinal directions and ensure accurate positioning of the rectangular iris with and without the sample. This is achieved with the aid of guide pins which are used to align the two sections of the chamber.

Photograph 1 shows the test chamber. It consists of two wave-

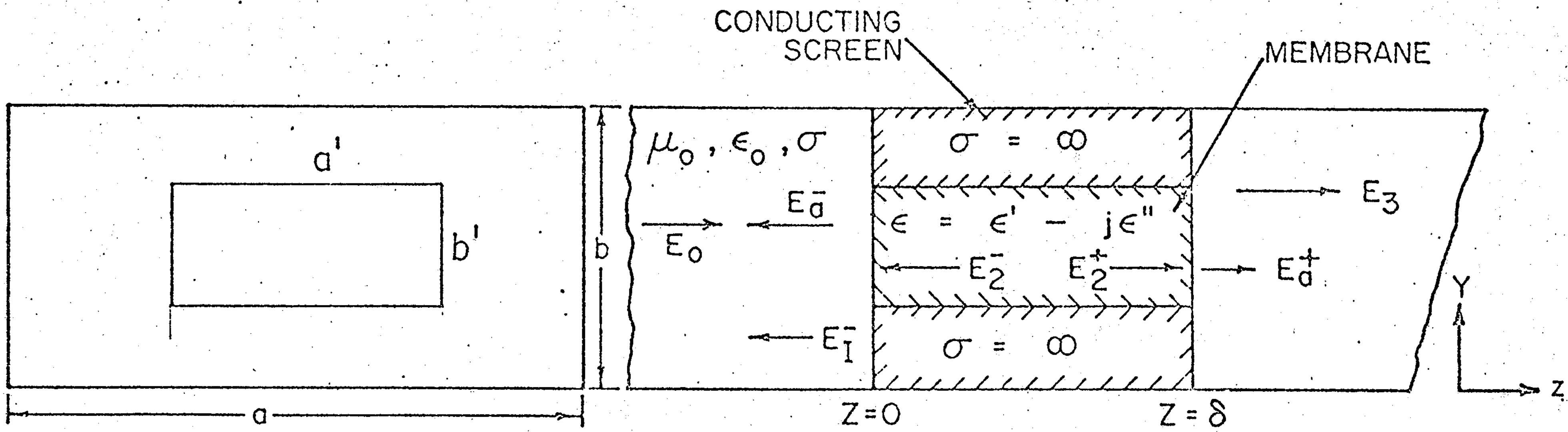

Fig. 1 CONDUCTING SCREEN WITH FILM APERTURE

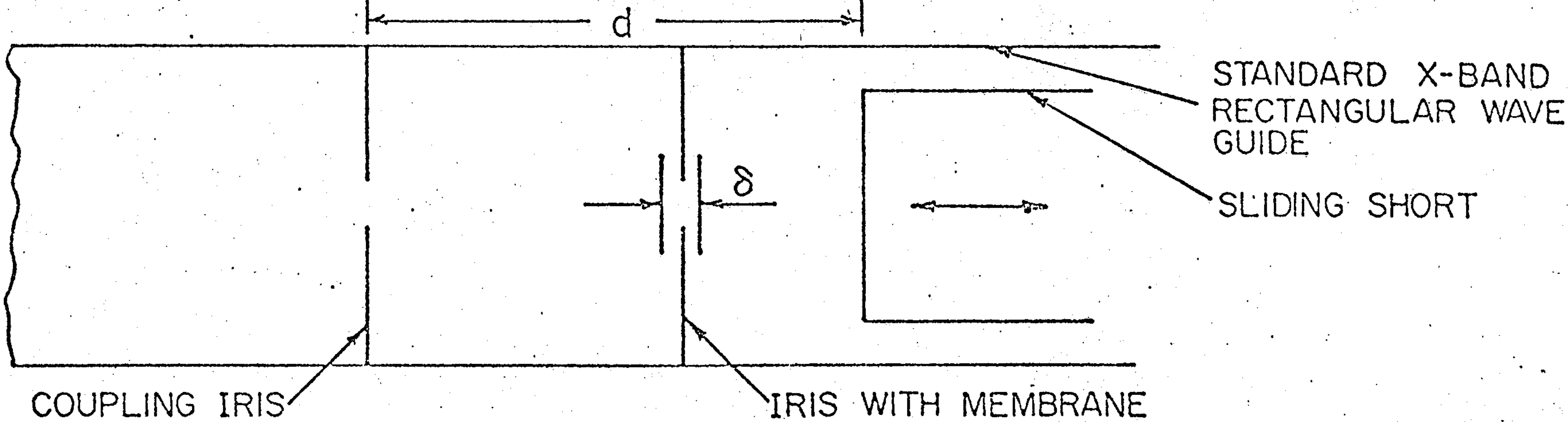

Fig. 2 RESONANT TEST CHAMBER

guide sections, one fixed and the other variable in length. The iris containing a sample in the aperture is placed between the two sections and the three parts are aligned with the help of pins on the fixed section. The cavity is coupled to the main waveguide through a circular iris of radius $\frac{15}{128}$".

For the sake of convenience in calculations some samples are prepared to extend over the whole cross section of the cavity (i.e. without the iris) while the other samples of the same material are suspended in the resonant iris. This provides a check on the calculated results and allows experimental determination of the shape factor γ associated with the resonant iris as will be discussed in section 3.4.

As has been mentioned in the introduction, the work presented here resulted from fundamental research on rf safety standards which involves the study of the rupture of the phospho-lipid membranes which resemble living tissues in their properties. Although the work described here concerns only measurement of dielectric constant of these membranes, the set up shown in Fig. 6 is also suitable for rupture test. In order to perform the rupture tests, the cavity may be placed in a temperature controlled chamber and connected to a medium power microwave generator and the measurement set up via an electrically controlled waveguide switch which changes the mode of operation from 'measurement' to irradiation.

<u>The Resonant Iris</u>:

<u>3.2 Theoretical Consideration</u>:

A metal diaphragm with a rectangular opening exhibits a susceptance-frequency characteristic similar to that of a parallel resonant circuit shunting the guide. In fact elements of a great variety of shapes may be made to resonate at any microwave frequency depending upon the dimensions of the element. A resonant element of the dumb-bell shape may be made with a number of variations as shown in Fig. 3. Tunable resonant elements can be made using posts, screws etc.

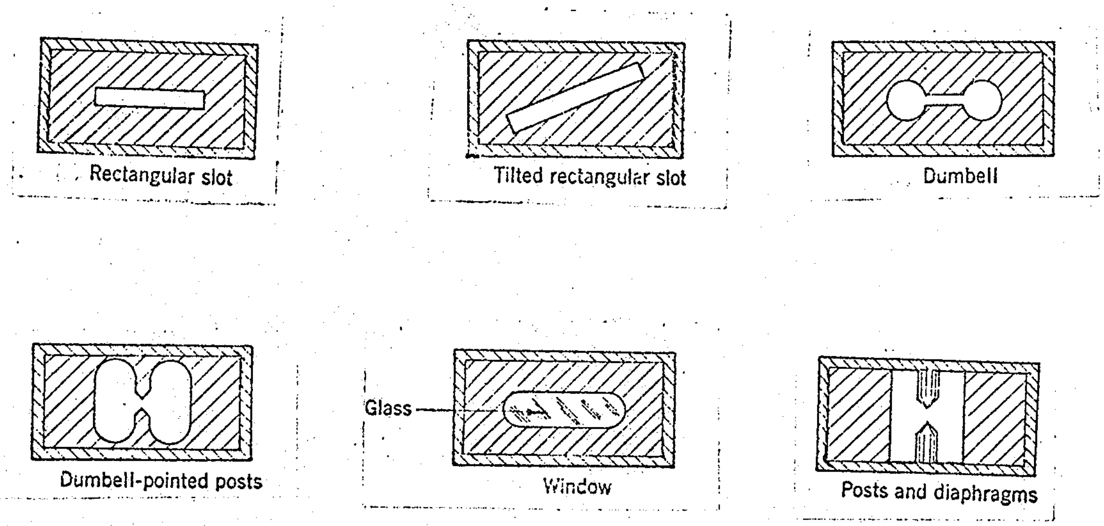

FIG. 3 RESONANT IRISES

To understand the behaviour of these elements, it is desirable to calculate the field in the junction so that one can know the dependence of the resonant frequency on the geometrical parameters of the elements, the frequency dependence of the transmission or reflection of power and also the energy dissipated in the element because of currents in the metal posts. Unfortunately, even the simplest resonant element-the rectangular slot-has not been analyzed theoretically to the extent of finding the field in the aperture. The method of attack at present is limited to finding experimentally the equivalent circuit of the resonant element. The equivalent circuit of a resonant iris has been derived in Appendix 2 and is helpful in understanding the behaviour of the iris.

3.3 Design of Rectangular Resonant Iris:

The approximate dimensions of a centrally located window in a rectangular guide operating in a dominant mode are given by the empirical relation given below [10].

$$\frac{a}{b}\sqrt{1-\left(\frac{\lambda}{2a}\right)^2} = \frac{a'}{b'}\sqrt{1-\left(\frac{\lambda}{2a'}\right)^2} \qquad (5)$$

where a and b are the guide dimensions, a' and b' are the dimensions of the opening (with a' measured parallel to a and b' parallel to b) and λ is free-space wavelength.

The design can be carried out in two ways. In one case the dimension b' is assumed and the corresponding value of a' is calculated for a given value of a, b and λ. The second method depends on a geometrical construction: In the centre of the cross section of the guide, lay out a line of length $\lambda/2$, parallel to larger dimension of the guide, and centered with respect to the walls as shown in Fig. 4. Two hyperbolas are now drawn with their axes parallel to the guide walls, passing through the ends of this line

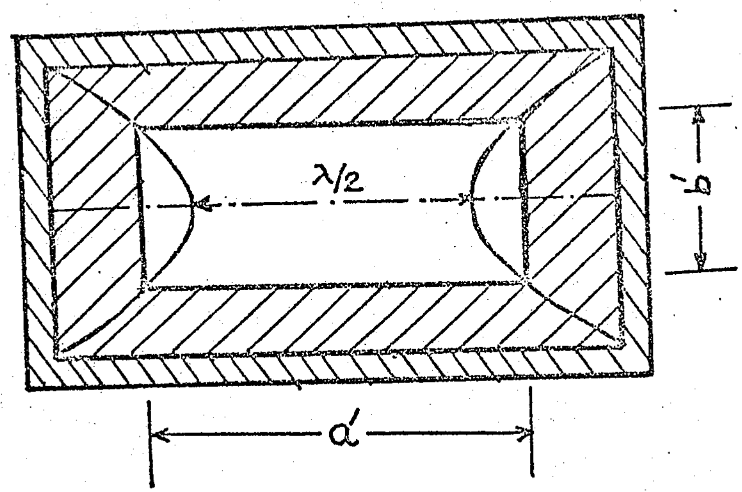

FIG. 4. DESIGN OF A RESONANT IRIS.

and also through the corners of the waveguide. All the centrally located rectangles whose corners fall on these hyperbolas will be found to resonate at the same frequency but will have a different normalized characteristic admittance or loaded Q, which will increase with decreasing height of the window and will also increase with increasing thickness of the diaphragm. The design carried out using equation 2, usually has an error of much less than 5 percent of the predicted value. The effect of thickness on the dimensions required for resonance is negligible as long as it is below 0.04λ.

Four rectangular resonant irises were designed to study the behaviour of their γ factor as described in section 3.4. The dimensions of these irises are given in Table 1. It has been proved that the resonant frequency of the iris of Figs. 5a and 5b are the same provided their areas are equal [9]. The four resonant irises used are shown in Photograph 2.

3.4 Shape Factor γ of the Resonant Iris:

It has been mentioned in Section 3.2 that the solution for the field in a rectangular iris is not available and is very difficult to determine. Therefore, it is necessary to devise some other means to evaluate the integral in the numerator of the right hand hand side of equations 1. This can be achieved by relating the field in the iris to the field in the waveguide without the iris. We define the ratio of these two fields by a shape factor called γ. It was observed experimentally that the shape factor is approximately constant for a given iris as long as the sample thickness is less than a few hundred microns. If γ is assumed to be constant, the ratio of the two fields will be observed as a proportional increase in the resonant frequency of the test chamber as can be seen from equation 1. This then gives a convenient method for determination of this shape factor.

Table 1

Dimensions of four resonant irises with resonant frequency = 10 GHz

Iris	a' in inches	b' in inches	c in inches
A	0.727	0.250	0.531
B	0.671	0.188	0.524
C	0.647	0.156	0.525
D	0.628	0.125	0.529

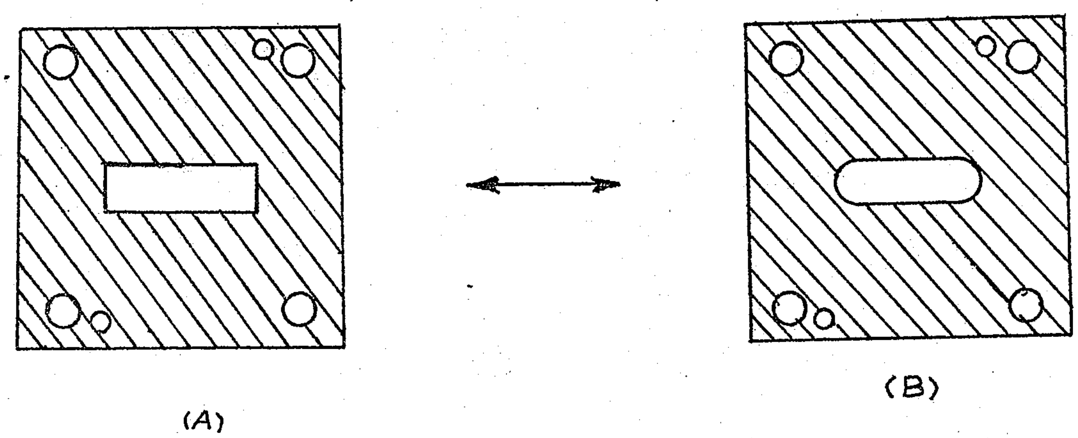

FIG. 5 RESONANT IRISES; RESONANT FREQ.=10 GHz.

Equal Aperture Areas

The measurement can be performed as follows: Place the loaded iris in the maximum longitudinal field in the cavity and adjust the variable short so that the cavity resonates at a given frequency (say 10 GHz), remove the sample and measure the shift in the resonant frequency. Now suspend the sample across the total cross-section of the cavity and adjust it for resonance at the same frequency as was used in the previous case (say 10 GHz). Measure the shift in the resonant frequency after removing the sample. The ratio of the two frequency shifts measured in this way determines the shape factor γ.

Table 2B gives the calculated shape factors for four rectangular irises, determined with three different sample materials. It can be observed that the γ factor is approximately constant as long as the frequency shift due to the sample, when suspended across the total cross-section of the waveguide, is below about 20 MHz. It may be mentioned here that even by using approximate methods for calculation of the field in the iris aperture, the error may be quite high.

Table 2B also gives β, the square root of the ratio of the cross-sectional areas of the waveguide to that of the iris aperture. It is expected that the shape factor γ should be equal to this β, since at resonance all the incident energy passes through the aperture. The discripency in the value of β and γ factors may be attributed to the fact that when the iris is removed from the chamber and the cavity length is readjusted for resonance, the sample is no more in the maximum longitudinal field, therefore,the resonant frequency shift in the second case is decreased by a small amount. This measured shape factor is used later to calculate the dielectric constant of thin films.

Table 2A

Measured Frequency shifts for evaluating Shape

factor γ for the irises A, B, C and D.

Sample	Thickness in cms	Frequency Shift in MHz				
		Without iris	With Iris B	With Iris B	With Iris C	With Iris D
Polyethelene	.0079	18.0	31.0	33.5	42.0	46.5
Polyethelene	.0029	8.0	13.5	14.5	19.0	21.0
Mica	.00285	18.0	30.0	34.0	42.0	47.0

Table 2B

Calculated shape factor for the Irises A,B,C, and D
using frequency shifts of Table 2A

Iris	β*	Shape factor γ using		
		Polyethelene thickness = .0079 cms	Polyethelene thickness = .0029 cms	Mica thickness = .00285 cms
A	1.410	1.72	1.69	1.67
B	1.690	1.86	1.81	1.89
C	1.887	2.34	2.38	2.34
D	2.142	2.58	2.63	2.61

$$* \quad \beta = \left[\frac{\text{Area of the waveguide cross-section}}{\text{Area of the Iris Aperture}}\right]^{1/2}$$

CHAPTER IV

EXPERIMENTAL SET-UP AND MEASUREMENTS

The experimental set-up used is shown in Fig. 6 and involves oscilloscopic display of the reflected power versus frequency for measuring the Q factor and the center frequency of the cavity by the reflected power method [8]. The microwave source is a backward wave oscillator (BWO) type HP 5690A which is capable of sweeping over the entire x-band in a period of .01 to 100 secs., depending upon sweep time vernier setting. Signals proportional to the power incident and reflected from the cavity are applied to the two channels of a dual trace oscilloscope through two directional couplers (10 dB coupling and 40 dB directivity) terminated in matched crystal detectors. The horizontal frequency scale of the oscilloscope is obtained by sweeping the horizontal axis with a voltage proportional to that used to frequency modulate the oscillator.

A precision type wavemeter (HP x 532A) is used to obtain a frequency marker to be used for measurement of frequency shifts and bandwidth of the test cavity. Since the 3 dB bandwidth for the test cavity (Q = 3000) is small (of the order of a few MHz at a centre frequency of 10 GHz), the sharpness of the marker and the precise calibration of the frequency scale are extremely important in deciding the ultimate accuracy of the Q measurement. Since the resolution of the wavemeter was only 5 MHz and the marker obtained was not sharp enough, it was decided to use a communication receiver in conjunction with a mixer and a local oscillator to obtain two sharp markers as explained below.

The modified set up uses an auxiliary frequency-stable klystron oscillator set at the resonant frequency of the cavity while the BWO in the

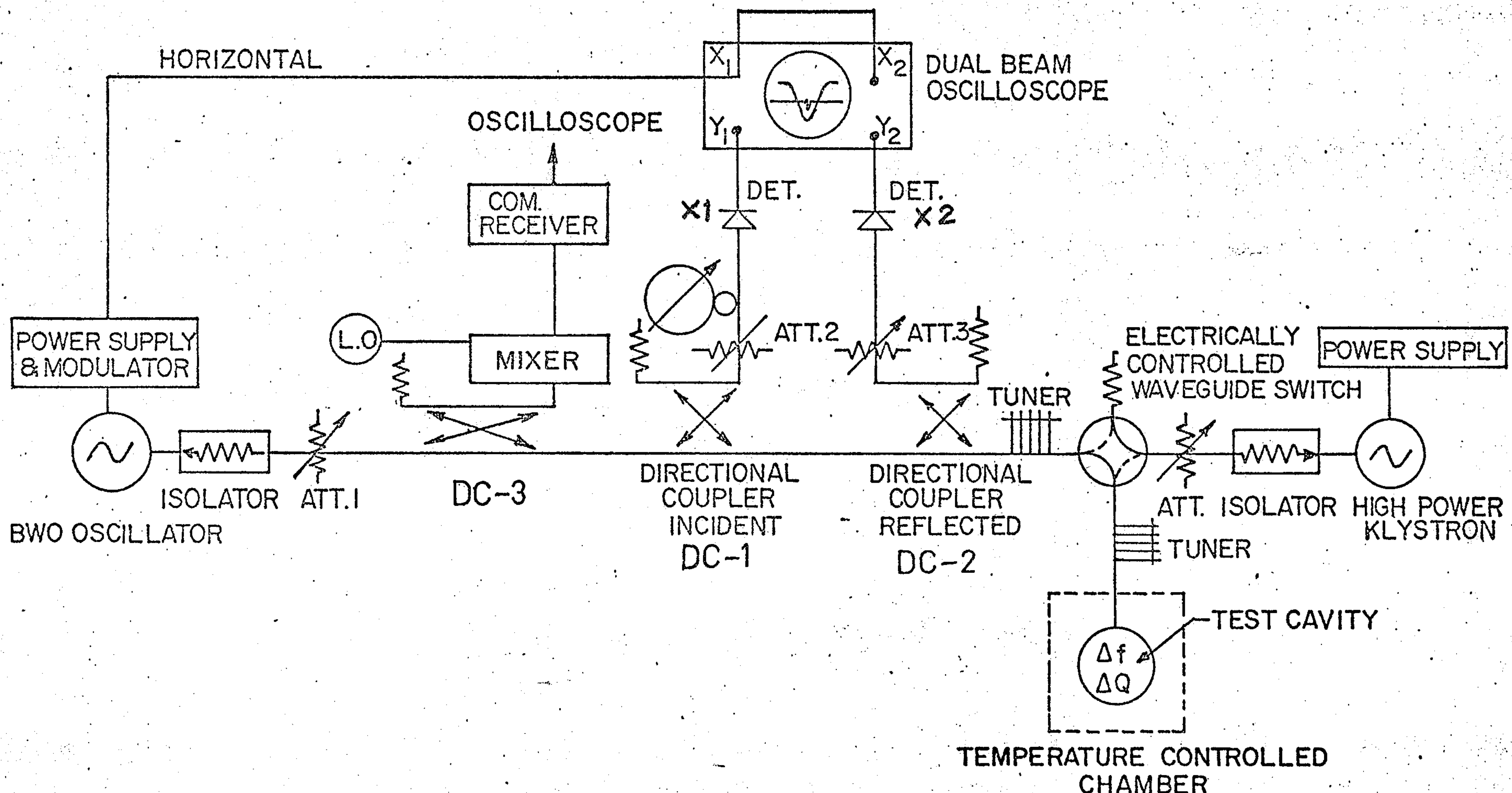

FIG. 6. MEASUREMENT SET – UP

main line is frequency swept between $f_o \pm \Delta f_s$ where Δf_s is the amount by which the center frequency changes during the sweep period. The incident signal is sampled by the directional coupler DC-3 and is mixed with the local oscillator signal. The output of the mixer is fed to a communication receiver which responds only to the difference signal from the mixer. A 10 KHz pip is obtained whenever the difference frequency corresponds to the dial setting of the receiver which occurs twice during each sweep cycle (positive and negative difference). Therefore the frequency separation between the two markers is twice the dial recording on the communication receiver.

The measurement procedure is outlined in the steps below:

1. Suspend the sample in the test chamber.
2. Adjust wavemeter to the desired center frequency 10 GHz.
3. Set the BWO in sweep mode with center frequency approximately 10 GHz.
4. Tune the test chamber so that the center frequency of the displayed curve is 10 GHz. This is achieved when the wavemeter response curve peak coincides with that of the test chamber.
5. Measure the Q of the response trace of the chamber as outlined in the next section.
6. Remove the sample from the test chamber.
7. Measure the shift in the peak of the response trace and also the Q of the cavity.

The shift in the resonant frequency and the change in the Q factor are now utilized to determine the complex dielectric constant of the sample as explained in Chapter V.

4.2 Measurement of Q factor of the chamber:

The procedure for the measurement of the Q factor as outlined in [8] is given below:

Calibration:

1. Adjust the BWO and wavemeter as explained in the previous section and obtain a response curve on the oscilloscope along with the two markers from the communication receiver.
2. Insert rf short at position B-B.
3. Set calibrated Att-2 at zero attenuation.
4. Bring rf power level to zero and with the aid of vertical centering controls bring the two baselines into coincidence.
5. Switch the rf power on and adjust Att-3 so that the reference and reflected traces coincide.
6. Check the 'tracking' of the two crystals x_1 and x_2 by varying Att-1 from 0 to 25 db. The two traces should coincide over the entire range.

Measurement of Q

1. Remove the shorting plate and tune the cavity to resonance at 10 GHz.
2. Lower the incident power trace so as to touch the 'shoulders' of the reflected power trace using attenuator Att-2, this reading on Att-2 gives $|\rho_1|^2$ in dB .
3. Measure $|\rho_o|^2$ in dB by lowering the incident power trace so as to touch the minimum point of the reflected power trace, using Att-2.
4. Choose a convenient value of $|\rho|^2$ and measure the bandwidth Δf by means of the two markers obtained from the communication receiver as explained in section 4.1

4.3 Digital Read-out method of Measurement of shift in Resonant frequency:

One of the main limitations of the method for testing very thin samples, in the range of a few microns, was the available resolution in the measurement of the shift in resonant frequency. So, to increase the reliability of measurement a modified set up as explained below was used.

In the modified set up the BWO oscillator is set at a fixed frequency of 10 GHz, rather than swept, and the loaded test chamber adjusted to resonate at the same frequency with the aid of a sliding short and a VSWR meter. The sample is then removed and the BWO frequency control readjusted so that the cavity resonates again. The new resonant frequency is then mixed with a 10 GHz signal from a phase locked local oscillator. The difference frequency is displayed on a digital frequency counter. Photograph 3 shows the set-up used for digital as well as analogue techniques.

CHAPTER V

CALCULATIONS AND EXPERIMENTAL RESULTS

5.1 Calculation of the Q-factor:

A sample calculation for the measurement of the Q of the empty test chamber is given below:

The values of $|\rho_0|^2$ and $|\rho_1|^2$ were measured to be 9 dB and 0.1 dB respectively. The 3dB bandwidth was found to be 3.0 MHz.

$$|\rho_1|^2 = \text{antilog } (-0.1/10) = 0.998$$

$$|\rho_0|^2 = \text{antilog } (-9/10) = 0.126$$

$$|\rho|^2 = 0.50$$

$$\alpha = \left[\frac{|\rho|^2 - |\rho_0|^2}{|\rho_1|^2 - |\rho|^2}\right]^{1/2} = \left[\frac{0.50 - 0.126}{0.998 - 0.50}\right]^{1/2} = .87$$

$$\text{and} \quad Q_L = \alpha(f_o/\ f) = \frac{.87 \times 10^{10}}{3 \times 10^6} = 2900$$

Where Q_L is the loaded Q of the cavity.

5.2 Calculation of Dielectric Constant:

In order to test the validity of the perturbation equation (1), measurements were carried out over a number of very think films of various materials of known dielectric constant. For each sample two sets of measurements were conducted, where the sample in one case was suspended over the total cross-section of the cavity and for the other in the iris aperture. Since for the materials tested the loss tangent is very small, only the real part of the dielectric constant ε_r was evaluated for which case the perturbation equation reduces to

$$2\,\frac{\Delta f}{f_s} = (\varepsilon_r - 1)\,\frac{\int_{v_s} \vec{E}_0 \cdot \vec{E}_2 \, dv}{\int_{v_o} |\vec{E}_0|^2 \, dv} \tag{6}$$

To determine the unknown ε_r, the ratio of the integrals needs to be evaluated. Since the sample is placed tangential to the electric field, the field $\vec{E}_2$ in the sample may be set equal to the unperturbed field $\vec{E}_0$ for very thin films extending over the total cross-section. The field $\vec{E}_2$ is assumed to be in the y direction, which is the same as for $\vec{E}_0$ since the dielectric is essentially loss-less and isotropic and has no effect on the polarization of the field.

The field distribution when the cavity is excited in the TE_{10n} mode is given by

$$E = E_{max} \,\mathrm{Sin}\,(\frac{\pi x}{a})\ \sin\,(\frac{\pi z}{d}) \tag{7}$$

Since the sample is placed where the electric field in the longitudinal direction is maximum, the field E_2 in the sample reduces to

$$E_2 = E_{max}\,\mathrm{Sin}\,(\frac{\pi x}{a}) \tag{8}$$

For a sample thickness δ and total cavity length d, the ratio of the integrals becomes $2\frac{\delta}{d}$ and therefore

$$\varepsilon_{r_1} = (\frac{\Delta f_1}{f_s})\,(\frac{d}{\delta}) + 1 \tag{9}$$

Where the subscript 1 denotes the case when the sample occupies the full cross-section of the cavity. For the case when the sample is in the iris aperture only, the subscript 2 is used and a geometrical factor or shape factor denoted by γ, is introduced as discussed previously, i.e.

$$\varepsilon_{r_2} = \left(\frac{\Delta f_2}{f_s}\right)\left(\frac{1}{\gamma}\right)\left(\frac{d}{\delta}\right) + 1 \qquad (10)$$

Table 3 presents results of the experimental procedure for thin films of polyethelene, plexiglass and mica. Fig. 7 shows an experimental plot of sample thickness vs. shift in resonant frequency for polyethelene samples which is a linear relationship as expected.

The results for the relative dielectric constant of phospholipid films deposited on glass substrates by a process of evaporation are given in Table 4. The relative dielectric constant averaged over three samples is approximately 2.08.

5.3 Conclusions:

The cavity perturbation method using a resonant iris to concentrate the field in the sample has been found to provide fairly accurate and reproducible results for frequency shifts as low as 2 MHz. For materials of relatively low dielectric constants, thicker samples have to be used, while in the case of high dielectric materials only relatively thin samples will be suitable for measurement (see Fig. 8).

One of the main limitations of the method for testing very thin samples, in the range of a few microns, is the available resolution for the measurement of the shift in resonant frequency. This difficulty can be partly overcome by using the digital technique described in section 4.4, but there still remains an ambiguity of about 1 MHz due to the chamber section, resulting from the use of screws,etc.

An effective method for improving the utility of the chamber to test very thin films, with little ambiguity, is to increase the field in the sample by using irises of higher Q and shape factors and to decrease the wall losses of the chamber by gold plating the cavity and the resonant

Table III

RESULTS FOR DIELECTRIC MEMBRANES

$f_s = 10$ GHZ $\qquad d = 1.5\lambda_g = 5.96$ cm $\qquad \gamma = 1.785$

$$\varepsilon'_r = \begin{cases} \left(\frac{\Delta f_1}{f_s}\right)\left(\frac{d}{\delta}\right) + 1 & \text{WITHOUT IRIS} \\ \left(\frac{\Delta f_2}{f_s}\right)\left(\frac{d}{\delta}\right)\frac{1}{\gamma} + 1 & \text{WITH IRIS} \end{cases}$$

SAMPLE	THICKNESS mm	ε'_r TABULATED	WITHOUT IRIS Δf_1 (MHZ)	WITHOUT IRIS ε'_r (MEASURED)	WITH IRIS Δf_2 (MHZ)	WITH IRIS ε'_r (MEASURED)
PLEXIGLASS	0.635	2.49	154	2.456	277	2.481
POLYETHYLENE	0.178	2.25	38	2.280	68	2.259
MICA	0.122	4.86	78	4.836	139	4.852

iris. An improvement in the chamber can be made by using a cylindrical cavity instead of the rectangular one used.

It is also necessary to find a suitable substrate material. Two possible materials are quartz and mica; quartz because it has a very low loss factor, and mica because it can be cleaved so thin that its losses are unimportant. Here, it may be noted that the dielectric constant of the substrate materials should be higher than that of the test film (but not so high as to violate the perturbation theory). This requirement is necessary to ensure that there is a maximum field concentration in the sample under test. Therefore, for choosing the proper substrate material an approximate value of the dielectric constant of the test sample should be known or measured.

Table IV

RESULTS FOR PHOSPHO-LIPID MEMBRANES

SAMPLE	THICKNESS mm	WITHOUT IRIS Δf_1 (MHZ)	WITHOUT IRIS ε'_r (MEASURED)	WITH IRIS Δf_2 (MHZ)	WITH IRIS ε'_r (MEASURED)
1	0.04			14.0	2.173
2	0.08			25.0	2.046
3	0.12			37.0	2.040
4	0.11	19.0	2.037		
5	0.011	2.0	2.090		

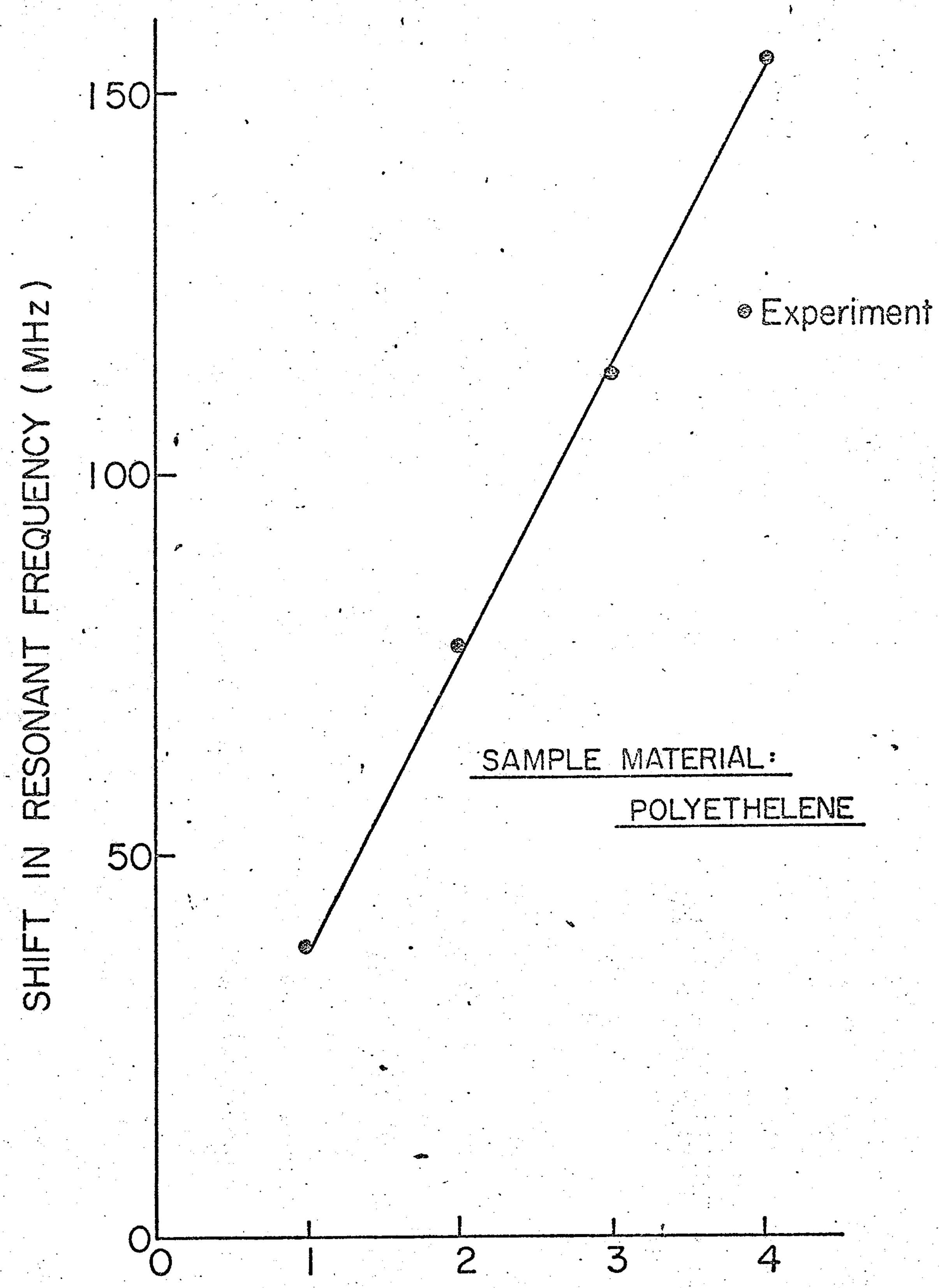

FIG.7.

CHANGE OF RESONANT FREQUENCY WITH SAMPLE THICKNESS

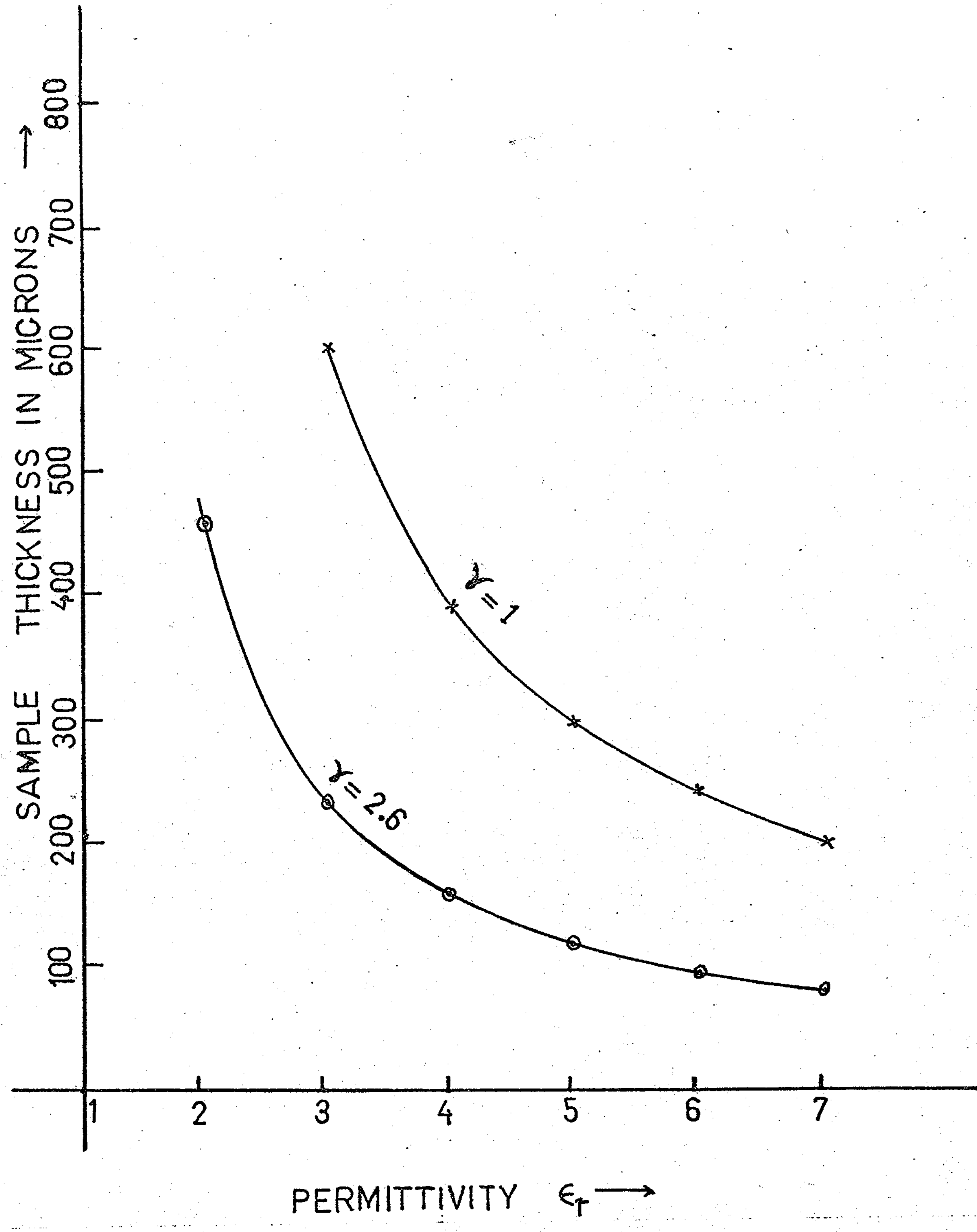

FIG. 8 SAMPLE THICKNESS Vs. PERMITTIVITY FOR A RESONANT FREQ. SHIFT OF 2.0 MHz.

APPENDIX I

DERIVATION OF THE PERTURBATION EQUATION:

Consider a resonant cavity whose walls are assumed to be lossless. Maxwell's equations for this cavity may be written as:

$$\nabla \times \vec{E}_1 = -j\omega_1\mu_0\vec{H}_1 \qquad \text{[A1.1a]}$$

$$\nabla \times \vec{H}_1 = j\omega_1\varepsilon_0\vec{E}_1 \qquad \text{[A1.1b]}$$

where the angular frequency ω_1 is complex $(\omega_R + j\omega_i)$, and reflects all losses including those of the coupling mechanisms. $\vec{E}_1$ and $\vec{H}_1$ are the electric and magnetic fields, respectively, in the cavity and ε_0 and μ_0 represent permittivity and permeability, respectively, of air.

When the sample is suspended in the cavity, the fields are perturbed by a small amount. Let us represent the new values of the electric and the magnetic field by $\vec{E}_2$ and $\vec{H}_2$, respectively. Then for this case Maxwell's equations are given by

$$\nabla \times \vec{E}_2 = -j\omega_2\mu_2\vec{H}_2 \qquad \text{[A1.2a]}$$

$$\nabla \times \vec{H}_2 = j\omega_2\varepsilon_2\vec{E}_2 \qquad \text{[A1.2b]}$$

where ε_2 is the permittivity of the sample material and ω_2 the new complex angular frequency.

Now by taking suitable dot products with eqs. [A1.1] and [A1.2], subtracting and integrating over the cavity volume, we obtain

$$\int_{V_c} \{[\vec{E}_2 \cdot (\nabla \times \vec{H}_1) - \vec{E}_1 \cdot (\nabla \times \vec{H}_2)] + [\vec{H}_2 \cdot (\nabla \times \vec{E}_1) - \vec{H}_1 \cdot (\nabla \times \vec{E}_2)]\} \, dv$$

$$= j \int_{V_c} [(\omega_1\varepsilon_0 - \omega_2\varepsilon_2) \vec{E}_1 \cdot \vec{E}_2 - (\omega_1\mu_0 - \omega_2\mu_2) \vec{H}_1 \cdot \vec{H}_2] \, dv \qquad \text{[A1.3]}$$

The left hand side of equation [A1.3] can be written as a difference of two terms of the form $\nabla \cdot (\vec{H} \times \vec{E})$ so that on employing Gauss's divergence theorem and bearing in mind that the cavity surface is assumed to be perfectly conducting, we can prove that the left hand side is equal to zero. Therefore from eq. [A1.3] we get

$$\omega_1 \int_{V_c} (\varepsilon_0\vec{E}_1 \cdot \vec{E}_2 - \mu_0\vec{H}_1 \cdot \vec{H}_2) \, dv = \omega_2 \int_{V_c} (\varepsilon_2\vec{E}_1 \cdot \vec{E}_2 - \mu_2\vec{H}_1 \cdot \vec{H}_2) \, dv \qquad \text{[A1.4]}$$

When each side of eq. [A1.4] is subtracted from the integral:

$$\omega_2 \int_{V_c} (\varepsilon_0\vec{E}_1 \cdot \vec{E}_2 - \mu_0\vec{H}_1 \cdot \vec{H}_2) \, dv$$

and the terms are rearranged, we get,

$$\frac{\omega_2 - \omega_1}{\omega_2} = \frac{\int_{V_c} (\mu_2 - \mu_0) \vec{H}_1 \cdot \vec{H}_2 - (\varepsilon_2 - \varepsilon_0) \vec{E}_1 \cdot \vec{E}_2] \, dv}{\int_{V_c} (\varepsilon_0\vec{E}_1 \cdot \vec{E}_2 - \mu_0\vec{H}_1 \cdot \vec{H}_2) \, dv} \qquad \text{[A1.5]}$$

Now for a small perturbation due to the sample, this equation becomes

$$\frac{\omega_2 - \omega_1}{\omega_2} \doteqdot \frac{(\mu_2 - \mu_0) \int_{V_s} \vec{H}_1 \cdot \vec{H}_2 \, dv - (\varepsilon_2 - \varepsilon_0) \int \vec{E}_1 \cdot \vec{E}_2 \, dv}{2\varepsilon_o \int_{V_c} |\vec{E}_1|^2 \, dv} \qquad \text{[A1.6]}$$

The integration in the numerator of equation [A1.6] is over volume V_s since $\varepsilon_2 = \varepsilon_0$ and $\mu_2 = \mu_0$ over cavity except in small volume V_s. When the sample is non magnetic we have $\mu_2 = \mu_0$. Therefore eq. [A1.6] becomes

$$\frac{\omega_2-\omega_1}{\omega_2} = -\frac{\varepsilon_r - 1}{2} \frac{\int_{V_s} \vec{E}_1 \cdot \vec{E}_2 \, dv}{\int_{V_c} |\vec{E}_1|^2 \, dv} \qquad \text{[A1.7]}$$

where ε_r is the complex dielectric constant of the sample. Substituting for the complex angular frequencies ω_1 and ω_2 in eq. [A1.7] in terms of the measureable quantities Q and resonant frequencies, we get

$$2 \left| \frac{f_{r_1} - f_{r_2}}{f_{r_2}} \right| - j \left| \frac{1}{Q_{L_1}} - \frac{1}{Q_{L_2}} \right| = (\varepsilon_r - 1) \frac{\int_{V_s} \vec{E}_1 \cdot \vec{E}_2 \, dv}{\int_{V_c} |\vec{E}_1|^2 \, dv} \qquad \text{[A1.8]}$$

Here the field $\vec{E}_1$ in the empty cavity is presumed to be known and only field $\vec{E}_2$ in the sample volume is to be evaluated.

APPENDIX 2

THE EQUIVALENT CIRCUIT OF A RESONANT IRIS

A resonant iris may be represented by a lumped inductance, capacitance, and conductance shunted across the line as shown in Fig. 9 [10]. The susceptance B of the equivalent circuit of the resonant element may be defined by

$$B = \omega C - \frac{1}{\omega L} \qquad [A2.1]$$

and the resonant frequency is given by

$$\omega_o^2 = \frac{1}{LC} \qquad [A2.2]$$

we define the loaded Q_L as,

$$Q_L = \frac{\omega_o}{\omega_2 - \omega_1} \qquad [A2.3]$$

where ω_1 and ω_2 are the frequencies, at which the susceptance equals plus and minus the total conductance, and are given by

$$\omega_2 C - \frac{1}{\omega_2 L} = +(2y_o + G) \qquad [A2.4]$$

$$\omega_1 C - \frac{1}{\omega_1 L} = -(2y_0 + G) \qquad [A2.4b]$$

If the positive roots of eqs. [A2.4] are chosen

$$Q_{L_2} = \frac{\omega_o C}{2y_o + G} \qquad [A2.5]$$

Note that equation [A2.4] gives the frequencies at which half of the power is transmitted by the resonant iris. Let us now calculate the power reflection at ω_2. Equation [A2.4a] may be written as

$$B = 2y_o + G \tag{A2.6}$$

The admittance at frequency ω_2, looking from left to right at x-x in the circuit of Fig. 9, is given by

$$Y = Y_o + G + j(2Y_o + G) \tag{A2.7}$$

The reflection coefficient is then

$$\Gamma = - \frac{G + j(2Y_o + G)}{2Y_o + G + j(2Y_o + G)} \tag{A2.8}$$

from which the power reflection coefficient is

$$|\Gamma|^2 = \frac{G^2 + B^2}{(2Y_o + G)^2 + B^2} \tag{A2.9}$$

The expression for B in terms of r, the voltage reflection coefficient, is given by

$$B = \left[\frac{(Y_o^2 + Y_o G)\ (r - 1)^2 - rG^2}{r}\right]^{1/2}, \quad r \geq 1 \tag{A2.10}$$

A measurement of r at the resonant frequency, e.i. at the frequency for which $B = 0$, can be used to determine G

$$G = Y_o(r-1), \qquad r \geq 1 \tag{A2.11}$$

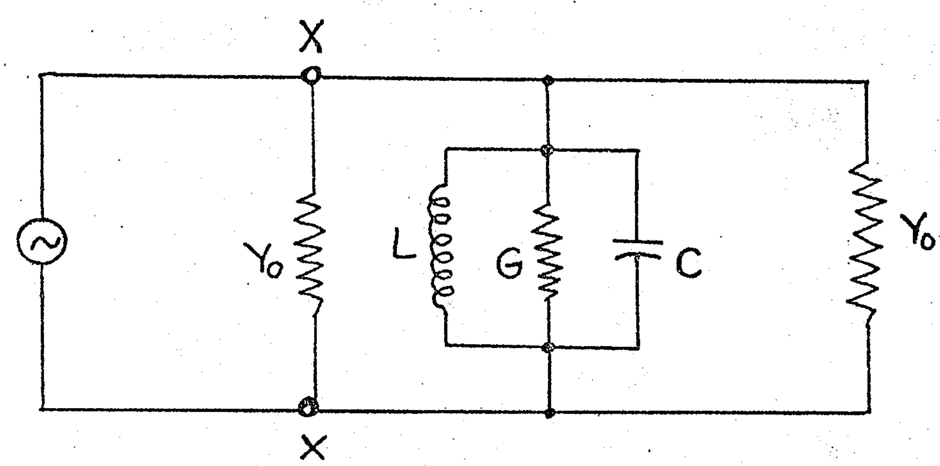

FIG. 9 EQUIVALENT CIRCUIT OF A RESONANT IRIS

BIBLIOGRAPHY

[1] Illinger, K.H. (1969): "Molecular Mechanisms for Microwave Absorption in Biological Systems", Symposium on the Biological Effects and Health Implications of Microwave Radiation, Sept. 17-19, Richmond, Virginia, U.S.A.

[2] Petkau, A. et. al. Biochemical Biophysical Acta, 203 (1970) 34.

[3] Bhar, J.N.: "Microwave Techniques in the Study of Semiconductors", Proc. IEEE, 1963, vol. 51, p. 1625.

[4] Jacobs, H., Brand, A.F., Meindle, J.D., Benanti, M. and Benjamin, R.: "Electrodeless measurement of semi Conductor resistivity at microwave frequencies", Proc. IRE, 1961, vol. 49, pp. 928 - 932.

[5] Nag, B.R. and Roy, S.K.: "Microwave measurement of Conductivity and dielectric constant of Semi Conductors", Proc. IEEE, 1963, vol. 51, p. 962.

[6] Gunn, M.W. and Brown, J.B.: "Measurement of semiconductor properties in a slotted-waveguide structure", Proc. IEE, 1965, vol. 112 (3), pp. 463 - 468.

[7] Champlin, K.S. and Krongard, R.R.: "The Measurement of Conductivity and permittivity of semi conductor spheres by an extention of cavity perturbation technique", IRE Trans., 1961, MTT-9, pp. 545 - 551.

[8] Sucher and Fox Handbook of Microwave Measurements, vol. II, Polytech. Press P.I.B., 1963.

[9] Stuchly, S.S. et.al, : "Wide band Rectangular to Circular Waveguide Mode and Impedance Transformer, IEEE Trans., MTT-13, no. 3, May 1965

[10] Smullin, L.D. and Montgomery, C.G.: "Microwave Duplexers", Radiation Lab. Series, vol. 14, McGraw Hill Book Company, 1948.

[11] Ramey, R.L. et. al.: "Microwave Properties of Thin Films with apertures", IEEE Transactions, MTT-18, no. 4, April 1970, p. 196.

[12] Gunn, M.W. et.al.: "Wave Propagation in Rectangular Waveguides with Semiconducting Wall", Proc. IEE, vol. 115, no. 1, Jan. 1968, p. 32.

[13] Shaw, T.M. and Windle, J.J.: "Microwave Techniques for the Measurement of the Dielectric Constant of Fibers and Films of High Polymers", J. Appl. Phys., vol. 21, Oct. 1950, p. 956.

[14] Champlin, K.S. and Armstrong, D.B.: "Waveguide Perturbation Techniques in Microwave Semiconductor Diagnostics", IEEE Transactions, 1962, MTT-11, p. 73.

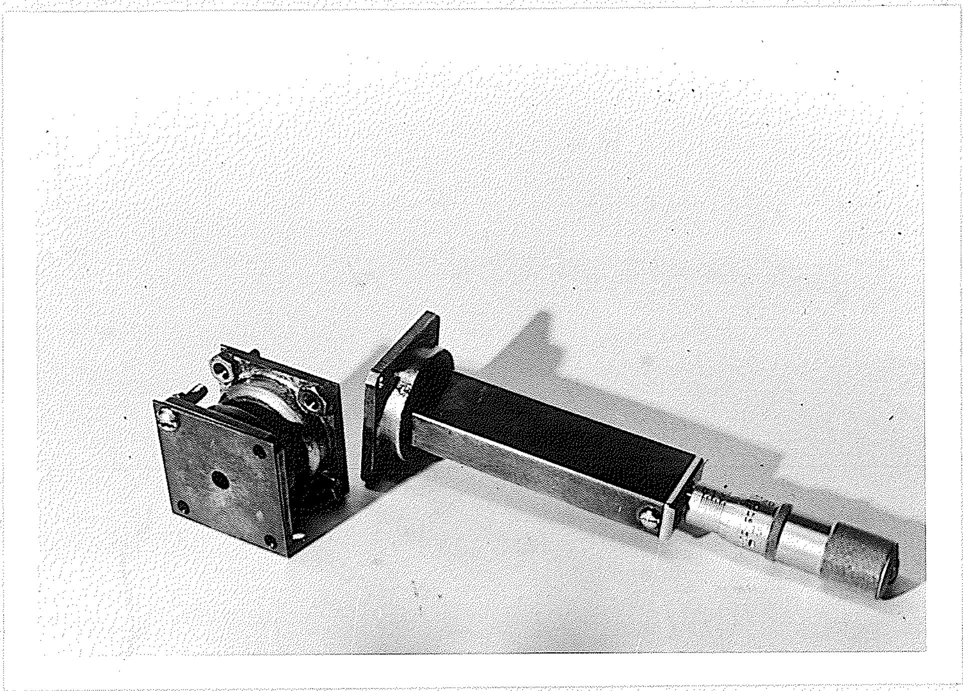

Photograph 1a, Test Chamber

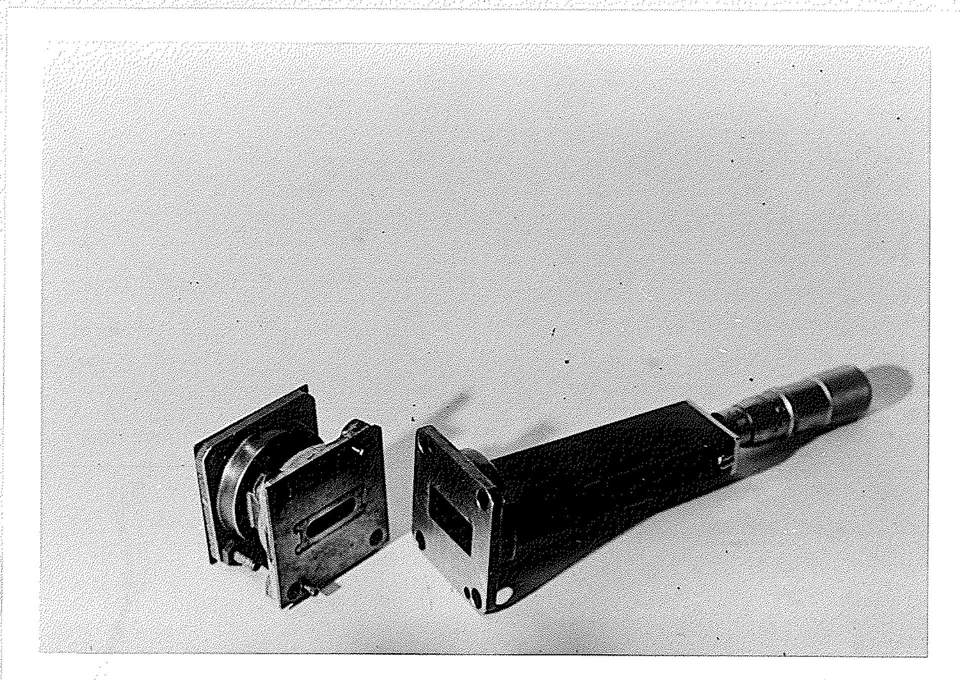

Photograph 1b. Test Chamber

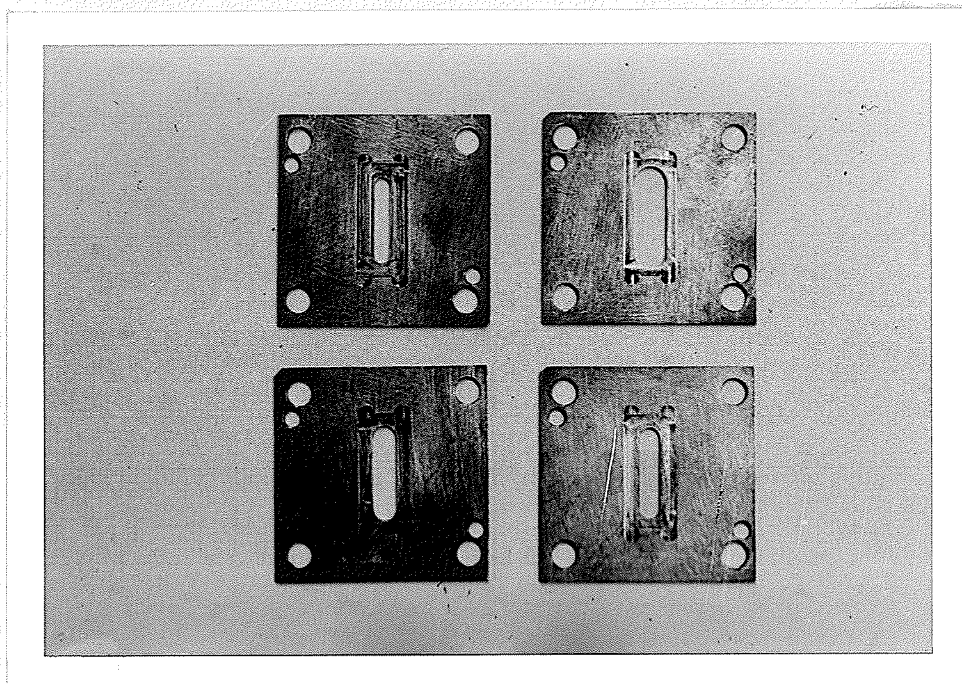

Photograph 2. Resonant Irises

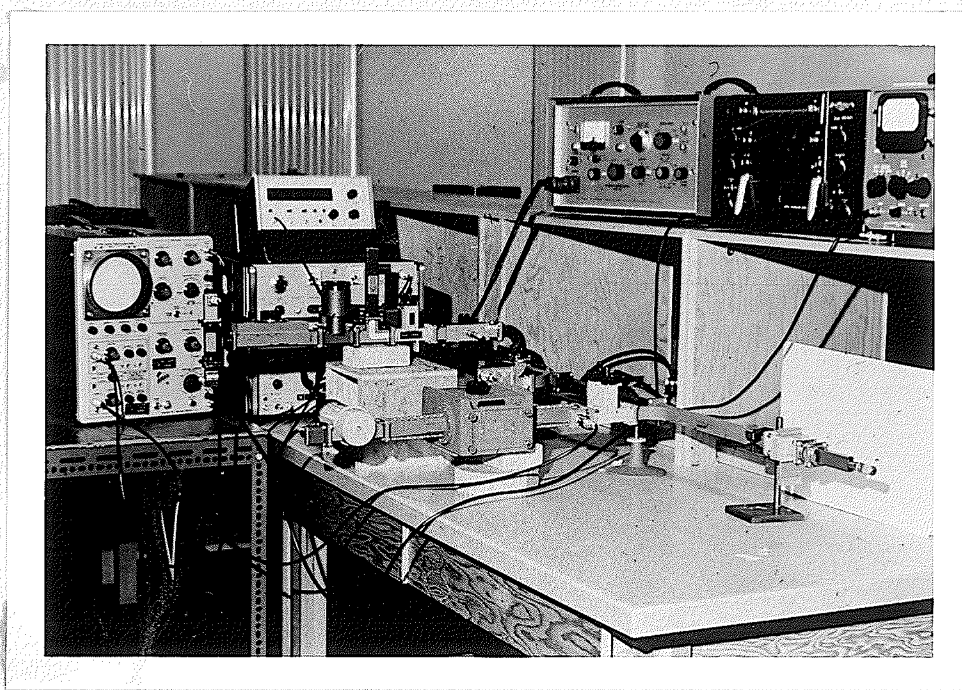

Photograph 3 Experimental Set-up